

ANOMALOUS *p*-SHELL ISOSCALAR MAGNETIC MOMENTS: REMEASUREMENT OF ⁹C AND THE INFLUENCE OF ISOSPIN NONCONSERVATION

M. Huhta, P.F. Mantica, D.W. Anthony, B.A. Brown, B.S. Davids, R.W. Ibbotson, D.J. Morrissey, C.F. Powell, and M. Steiner

The ground state *g* factors of the proton-drip line nuclei ⁹C and ¹³O have been measured using spin-polarized radioactive beams and the technique of nuclear magnetic resonance on beta-emitting nuclei (β -NMR), and the results have been reported at recent conferences [1,2]. The deduced ground state magnetic moments of ⁹C and ¹³O, (-)1.3914(5) μ_N and (-)1.3891(3) μ_N , respectively, are significantly quenched with respect to the single-particle Schmidt limit value of -1.91 μ_N expected for a pure $\nu p_{3/2}$ ground state. While the magnetic moment of ¹³O was shown to agree with simple shell model predictions using Cohen-Kurath wave functions [2], the same calculations were unable to reproduce the small magnetic moment value of ⁹C. This anomalous value, if verified, may be an indication of unique structure phenomena for the proton drip-line nucleus ⁹C ($S_p = 1.3$ MeV).

The isoscalar spin expectation value $\langle\sigma\rangle$ where

$$\langle\sigma\rangle = \frac{\mu(T_z = +1/2) + \mu(T_z = -1/2) - J}{\mu_p + \mu_n - 1/2}$$

has been shown to be a sensitive probe of deviations in the magnetic moments of light, mirror nuclei [3]. The $\langle\sigma\rangle$ values for $T = 1/2$ mirror nuclei up to $A = 41$ are shown in Fig. 1. The trends in these values away from the extreme single-particle estimates can be explained by considering core polarization. The $\langle\sigma\rangle$ deduced from the ¹³B - ¹³O mirror pair compares favorably with the observed trends in the $\langle\sigma\rangle$ values extracted for $T = 1/2$ nuclei. The $\langle\sigma\rangle$ value of 1.44 determined for ⁹Li - ⁹C, also shown in Fig. 1, lies well outside the $T = 1/2$ systematics.

We have remeasured the ground state *g* factor ⁹C ($T_{1/2} = 127$ ms) using the β -NMR technique and a primary beam and target combination different from [2] to confirm the anomalous value of the magnetic dipole moment of this nuclide. A secondary beam of spin-polarized ⁹C was produced by the fragmentation of ²⁰Ne projectiles at 80 MeV/nucleon in a 107 mg/cm² thick ⁹³Nb target. The spin-polarized ⁹C fragments were collected at +2.5° relative to the primary beam axis and separated using the A1200 fragment separator. The A1200 was set to select the peak of the momentum yield curve for ⁹C fragments with a momentum acceptance of 1% determined by slits placed at the first dispersive image of the device. A 425 mg/cm² Al degrader wedge was placed at the second dispersive image to separate fragments with a given *A/Z* ratio. Fragments were identified both at the A1200 focal plane and the experimental endstation by means of the energy loss in 300 μ m Si PIN detectors and the fragment time-of-flight relative to the K1200 Cyclotron radiofrequency (RF). The ⁹C fragments were implanted in a 250- μ m thick annealed Pt foil located at the center of the β -NMR apparatus. The spin-lattice relaxation time T_1 for the ⁹C in Pt system is estimated from theoretical band structure calculations [4] to be $T_1 > 200$ ms at 298 K.

The resonance curve obtained for ⁹C is shown in Fig. 2. The data were collected using the multiple adiabatic fast passage technique with continuous beam implantation [5]. In this method, the fragments of interest are continuously implanted while a frequency-modulated (± 10 kHz) RF signal is applied to the sample. A reference signal is collected in a succeeding run with no RF signal applied to the sample. This acquisition method allows for a 100% duty cycle, which is crucial in low count rate experiments such as the one described here, during which the ⁹C implantation rate was only 2 ions/s.

The data were fitted using a Lorentzian peak shape with a peak centroid of 892(2) kHz and a width of 5 kHz. Using the relation $h\nu_L = g\mu_N B$, where ν_L is the Larmor frequency, $B = 0.1257$ T and $I = 3/2$, we obtained a value of $1.396(3) \mu_N$ for the ${}^9\text{C}$ ground state magnetic dipole moment. The corrections for diamagnetic shielding and the Knight shift for the carbon in platinum system, given in Ref. [2], are smaller than the statistical error in our value for the magnetic moment of ${}^9\text{C}$. Therefore, these corrections have only been included in the overall error.

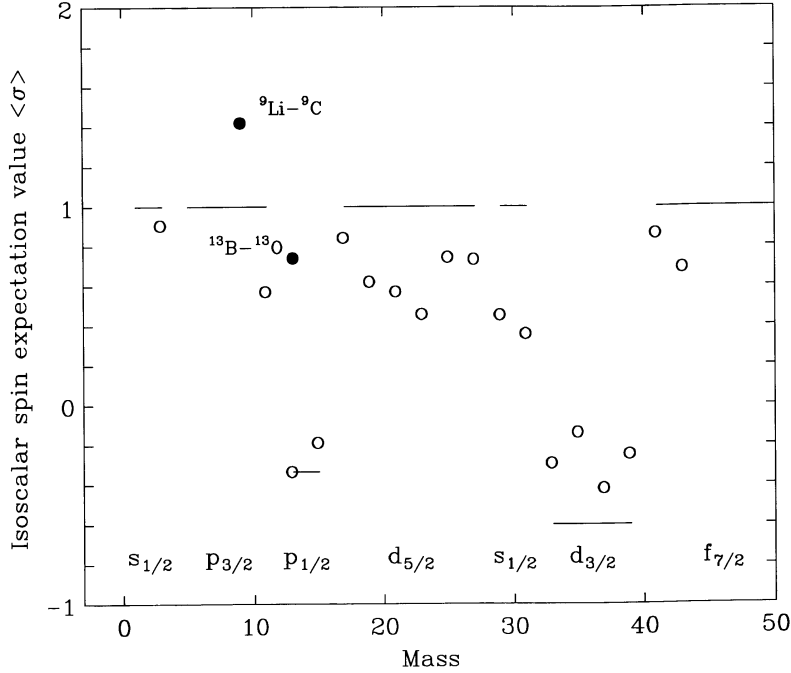


Figure 1: Isoscalar spin expectation values for $T = 1/2$ mirror nuclei (open circles). The solid lines indicate the values predicted by the extreme single particle model. The $\langle\sigma\rangle$ values deduced for the known $T = 3/2$ mirror partners are also shown (filled circles).

Our new measurement is in reasonable agreement with the previous value [1,2] of $(-1.3914(5)\mu_N)$ for the magnetic dipole moment of ${}^9\text{C}$, once again suggesting the unique character of this nucleus. We have performed shell model calculations for ${}^9\text{Li}$ and ${}^9\text{C}$ in an attempt to reproduce the quenched g factor of ${}^9\text{C}$ and the large $\langle\sigma\rangle$ extracted for the ${}^9\text{Li} - {}^9\text{C}$ $T = 3/2$ mirror pair. The PTBME interaction of Julies, Richter, and Brown [6], which includes a mass dependence for the two-body matrix elements, was chosen as it reproduces well the level energies and static electromagnetic moments of $0p$ -shell nuclides. We employed the simpler, bare g -factors for calculating the magnetic dipole moments of the ${}^9\text{Li} - {}^9\text{C}$ and ${}^{13}\text{B} - {}^{13}\text{O}$ mirror pairs as the results with effective g -factors were only slightly different from those derived with the bare nucleon values. The results of the shell model calculations are compared with the experimental magnetic moments and other recent theoretical calculations [7,8] in Table I. The shell model calculations reproduce the experimental magnetic moments and $\langle\sigma\rangle$ for the $A = 13$ $T = 3/2$ mirror partners. The calculated magnetic dipole moment of $-1.44 \mu_N$ for ${}^9\text{C}$ contains a significant contribution from the proton intrinsic spin, suggesting a breaking of paired proton spins as was observed in the AMD calculations [8]. The derived value of $\langle\sigma\rangle = 1.09$ for the $A = 9$ $T = 3/2$ partners, although greater than unity, is still well below the experimental value of $\langle\sigma\rangle = 1.44$.

To explore further the large value of $\langle\sigma\rangle$ for the ${}^9\text{Li} - {}^9\text{C}$ mirror pair, we extended the shell model calculations described above to include the isospin-nonconserving (INC) processes outlined by Ormand and Brown [9]. The Coulomb interaction should play a significant role in the low-energy

structure of loosely bound nuclei near the proton drip-line, and it is important to consider isospin mixing in these systems. The INC interaction of Ormand and Brown is composed of several parts: (1) the isovector single-particle energies for the $p_{1/2}$ and $p_{3/2}$ orbitals (two parameters), (2) the Coulomb matrix elements calculated with harmonic-oscillator radial wave functions are scaled by one overall strength parameter, (3) an isovector contribution to the strong interaction which is scaled to the isospin-conserving matrix elements by one parameter and (4) an isotensor contribution to the strong interaction which is scaled to the isospin-conserving matrix elements by one parameter. The strengths associated with these five parameters are determined by a least squares fit to 15 b coefficients and 7 c coefficients of the IMME for p -shell configurations in the mass region $A = 9 - 15$, which includes the binding energy data for the $A = 9$ $T = 3/2$ states studied in this experiment. Although the Coulomb interaction is scaled by a parameter, its value is within a few percent of that expected for the Coulomb interaction between protons. The isovector interaction (-4.2 percent of the isospin-conserving interaction) is required in order to understand the well known Nolen-Schiffer anomaly for the mirror displacement energies (the b coefficients). The resulting fit reproduces the experimental b coefficients to within 70 keV (rms) and the experimental c coefficients to within 13 keV (rms).

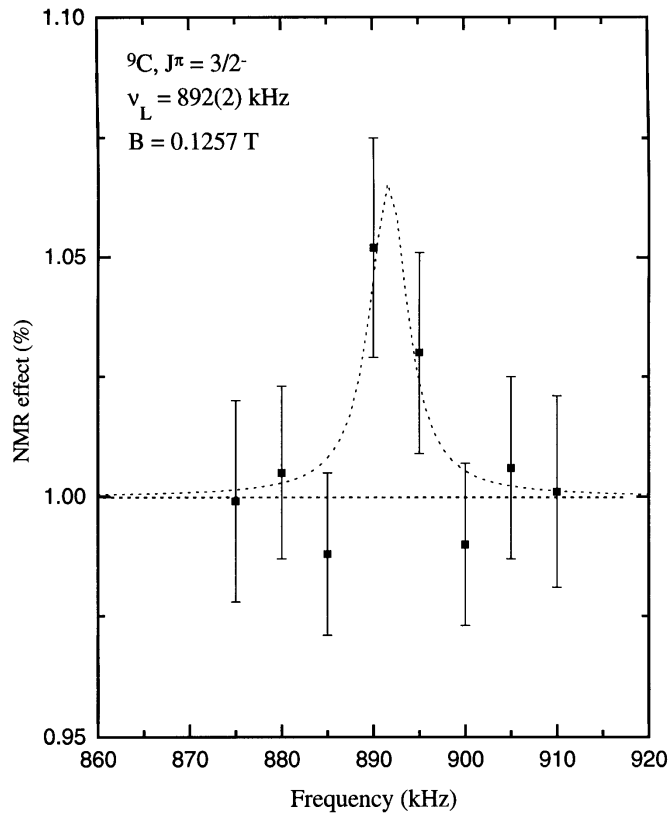


Figure 2: Resonance curve obtained for ${}^9\text{C}$. The frequency modulation for each point is ± 10 kHz of the central frequency using a triangle waveform with a 500 Hz repetition rate.

The INC wave functions are obtained in proton-neutron formalism and used to calculate the magnetic moments of the states of interest. For the $A = 9$ $T = 3/2$ states, the INC interaction allows mixing with the $T = 5/2$ states at higher energy. The isospin for the $A = 13$ $T = 3/2$ states is the highest allowed within the p -shell and thus they remain pure in isospin. We have investigated the importance of the four different terms discussed above. Of these the isovector interaction (3), gives the largest change in the $\langle \sigma \rangle$ value.

The results of the calculations employing the PTBME interaction and INC interactions are given in Table I. The present calculations result in a $\langle\sigma\rangle$ value of 1.18 for the ${}^9\text{C} - {}^9\text{Li}$ $T = 3/2$ mirror pair. Although we have demonstrated that the INC is important for the interpretation of mirror moments, the present calculations do not give the full effect observed experimentally ($\langle\sigma\rangle = 1.44$), but they go in the right direction. The effect is actually very small as can be observed by the change in values for the individual magnetic moments in Table I. It is only when the isoscalar magnetic moment is used to obtain the $\langle\sigma\rangle$ value that the effect becomes magnified.

Table 1: The magnetic dipole moments (in units of μ_N) for $T = 3/2$ mirror pairs.

Nuclide	Experiment	PTBME +	PTBME	Single Particle	Cluster Model	AMD
		INC				
${}^9\text{C}$	(-)1.3914(5)	-1.411	-1.437	-1.91	-1.50	-1.53
${}^9\text{Li}$	+3.4391(6)	+3.360	+3.350	+3.79	+3.43	+3.44
$\langle\sigma\rangle$	1.44	1.18	1.09	1.00	1.13	1.08
${}^{13}\text{O}$	(-)1.3891(3)	-1.355	-1.355	-1.91		
${}^{13}\text{B}$	+3.1771(5)	+3.126	+3.124	+3.79		
$\langle\sigma\rangle$	0.76	0.71	0.71	1.00		

The theoretical magnetic moments in Table I were obtained with harmonic-oscillator radial wave functions. It is possible to use more realistic Woods-Saxon or Hartree-Fock radial wave functions. However, they do not significantly change the result because the matrix element is diagonal and because the magnetic moment operator has no radial dependence. (There is a larger effect on the Gamow-Teller β decay matrix elements because it involves the off-diagonal overlap between proton and neutron radial wave functions.) The Coulomb contribution to the INC is also calculated with harmonic-oscillator radial wave functions, and we note that the present INC interaction is mainly determined from the rather tightly-bound nuclei in the upper p -shell where the harmonic-oscillator approximation may not be so bad. However, the use of harmonic-oscillator radial wave functions for the Coulomb matrix elements of the more loosely bound light p -shell nuclei (including ${}^9\text{C}$) may not be so good, and this may be a source of isospin asymmetry beyond the present model.

References

1. K. Matsuta et al., *Hyperfine Int.* **97/98**, 519 (1996).
2. K. Matsuta et al., *Nucl. Phys.* **A588**, 153c (1995).
3. K. Sugimoto, *J. Phys. Soc. Jap. Suppl.* **34**, 197 (1973).
4. K. Matsuta et al., *Hyperfine Int.* **97/98**, 501 (1996).
5. P. F. Mantica et al., *Phys. Rev. C* **55**, 2501 (1997).
6. R. E. Julies, W. A. Richter, and B. A. Brown, *S. Afr. J. Phys.* **15**, 35 (1992).
7. K. Varga, Y. Suzuki, and I. Tanihata, *Phys. Rev. C* **52**, 3013 (1995).
8. Y. Kanada-En'yo and H. Horiuchi, *Phys. Rev. C* **54**, R468 (1996).
9. W. E. Ormand and B. A. Brown, *Nucl. Phys.* **A491**, 1 (1989).